Radiative zeros and extra neutral gauge bosons at lepton-hadron colliders

Gilles Couture*
Guelph-Waterloo Program for Graduate Work in Physics, Department of Physics, University of Guelph, Guelph, Canada N1G 2W1
(Received 8 August 1988)

We consider the process $e^{\pm}p \to e^{\pm}\gamma X$. In the first section, we look for radiative zeros and find that they are absent in $e^{-}p$ collisions but possibly observable in $e^{+}p$ collisions. In the second section we investigate the effects of the exchange of an extra neutral gauge boson on the process at hand. We find that, given appropriate cuts and using expected luminosities at the DESY ep collider HERA, a 2-standard-deviation effect could arise from a light neutral gauge boson. Z' masses up to $\sim 300\ \mathrm{GeV}/c^2$ could be probed at the 1-standard-deviation level.

I. INTRODUCTION

Lepton-hadron colliders offer the possibility of studying processes at very high center-of-mass energy in a relatively simple environment. They are a very interesting and useful middle-point between lepton colliders and hadron colliders. The latest of these machines, HERA at DESY, is expected to produce the first collisions by spring 1990. At this machine, one will be able to produce neutral and charged gauge bosons,[1] admittedly not as many as will be produced at lepton colliders tuned at the resonance. This can allow a first measurement of the anomalous magnetic moment of the W boson (κ) and probe deeply into the gauge structure of the standard model (SM). The Higgs boson will also be investigated via weak-boson fusion. New, heavy quarks[2] might be produced, mainly through photon-gluon fusion, and top-type quarks up to 120 GeV will be investigated. The electron offers a very simple probe for the measurement of quark distributions[3] and if leptons have structure, one might get a glimpse at this behavior.

On more exotic physics, HERA will offer an ideal setting for production of leptoquarks[4] via lepton-quark fusion. Heavy leptons, abundant in grand unified theories (GUT's), could also be produced with masses up to a few hundred GeV (Ref. 5). Furthermore, different asymmetries available could show signatures of extra gauge bosons, charged and neutral, for masses up to a few hundred GeV (Ref. 6). It is clear that lepton-hadron colliders offer a window to probe a very rich physics beyond the SM. In this paper, we want to investigate the processes

$$e^{\pm}p \to e^{\pm}\gamma X \ .$$

The advantage of these particular processes is that they have a large cross section. Therefore, one might try to impose some cuts to enhance the new physics one wants to study and be left with a measurable cross section. We will consider the processes from two very different points of view. First, in Sec. II, we will consider radiative zeros. These offer the possibility of measuring the electric charge of quarks and probe the gauge structure of the theory. Second, in Sec. III, we want to look at extra neutral gauge bosons. These have attracted a lot of attention over the last two years since most GUT's predict the existence of at least one extra neutral gauge boson. Admittedly, their masses are not very constrained from the theories but it is not inconceivable that some of these bosons are light, well below 1 TeV. We will not consider the direct production of such a boson, rather we will look at the effects of the exchange of a virtual boson.

II. RADIATIVE ZEROS

Radiative zeros were first discovered by Mikaelian, Samuel, and Sahdev[7] while they were considering the processes $pp \to W^{\pm}\gamma X$ and $p\bar{p} \to W^{\pm}\gamma X$. They realized that the photon could not be emitted at a given angle in the γW c.m. frame. What was more interesting, this critical angle, in a given frame, depended only on the charges of the particles involved and not on the masses or energy. Furthermore, it was also found that the appearance of a zero of radiation required the anomalous magnetic moment of the W boson (κ) to have its canonical value $=1$. This last requirement might have been a valuable mean of measuring κ, but recent calculations[8] indicate that the deviations induced by loop corrections in different models are too small (≤ 0.05) to be measured by radiative zeros. In addition, $p\bar{p}$ colliders are plagued by large backgrounds[9] that make a measurement of $\kappa \leq 4$ very difficult.

Then, Brodsky and Brown[10] and Brown, Kowalski, and Brodsky[11] explained the radiative zeros as the relativistic version of the absence of electric dipole radiation when particles with the same charge-to-mass ratio collide nonrelativistically. There is destructive interference between the different contributions to the process. This generalized radiative zeros to a much broader class of processes. It was shown that if particles have the canonical gyromagnetic ratio of 2 and all vertices are of the standard gauge-theoretic form, then one will observe a radiative zero in the emission of a photon provided all ratios

$$\frac{Q_i}{p_i \cdot q} \qquad (1)$$

are equal; where Q_i, p_i are the charge and momentum of the ith particle and q is the photon momentum. This ratio also implies that the particles involved have the same sign charges. For example, $e^+e^-\to e^+e^-\gamma$ cannot lead to a radiative zero while $e^-e^-\to e^-e^-\gamma$ will, as was first noticed in Ref. 11. Furthermore, if a neutral particle is emitted besides the photon, one will still observe a radiative zero if the neutral particle is massless and goes along the same direction as the photon. For example, in the process $e^-\gamma\to\nu W^-$ the neutrino cannot be emitted along the photon beam.

As mentioned above, the critical angle depends only on the charges of the particles involved, in a given frame. In the center-of-mass frame, for example, the conditions $Q_i/(p_i\cdot q)=Q_j/(p_j\cdot q)$ lead to two conditions:

$$\cos(\theta_c)=\frac{Q_i-Q_j}{Q_i+Q_j} \tag{2}$$

and

$$\frac{Q_i}{Q_j}=\frac{\sqrt{s}-2\bar{p}^{\,0}_j}{\sqrt{s}-2\bar{p}^{\,0}_i}\ , \tag{3}$$

where $\bar{p}^{\,0}_{i,j}$ is the energy of the outgoing ith, jth particle. The first condition defines the critical angle but does not guarantee a radiative zero. The second condition guarantees destructive interference. This last condition is not necessary in the sense that incomplete destructive interference will still take place and a "dip" should be observed at the critical angle if the condition is not imposed.

The critical angle is momentum independent in the sense that if the two incoming particles have the same momentum ratio, no matter what each particle momentum is, the critical angle will be constant. In lepton and photon interactions, for example, the c.m. frame is well defined since the particles carry the full momentum. Therefore, a zero of radiation should be easily observable as long as the two incoming particles have the same momentum ratio. Hadron interactions are more difficult because the partons do not carry a fixed momentum fraction. The c.m. frame will change with respect to the laboratory frame from one event to the other. The radiative zero could then be washed out, as was observed in Ref. 7.

Before considering the proton processes, we will concentrate on the parton level. Very useful information can be obtained from these subprocesses. We have four such processes. They are

$$e^+u\to e^+\gamma u\ , \tag{4a}$$

$$e^+d\to e^+\gamma d\ , \tag{4b}$$

$$e^-u\to e^-\gamma u\ , \tag{4c}$$

$$e^-d\to e^-\gamma d\ . \tag{4d}$$

From the charge requirement, we see that processes (4a) and (4d) can lead to radiative zeros. As the photon can radiate from any of the fermion legs, one has to consider 4 Feynman diagrams in QED, 8 in the minimal standard model (we neglect the Higgs-boson contribution since its coupling is proportional to the fermion masses and negligible) and 12 if one considers an extra neutral gauge boson. This is shown in Fig. 1. The calculation is straightforward but very tedious. The expression we obtained for the (amplitude)^2 is very long and not very illuminating. We shall not write it here.

We checked the amplitude as follows. It is very simple to go from

$$e^-u\to e^-\gamma u \quad\text{to}\quad e^-e^+\to e^-\gamma e^+\ .$$

All one has to do is change a few couplings. However, the second process is very well known and explicit expressions for the total (amplitude)^2 can be found in the literature. Certainly $e^-e^+\to e^-\gamma e^+$ can proceed via s and t channels. However, it can be argued convincingly that for energies far away from the possible resonances, the s-channel contribution is a very small fraction of the total cross section.[12] So, in the appropriate energy range, our amplitude should be very close to the leptonic process, provided we consider only photon exchange and change a few couplings. We performed a numerical comparison using an amplitude from the literature.[13] We found that the two amplitudes agreed to within 5% for the total cross sections on the energy range considered here. We also verified that the different distributions were also in very good agreement. The remaining slight differences can arise from lack of statistics in the Monte Carlo simulations or s-channel effects. This gave us some confidence in the expressions of our (amplitude).[2]

Consider Fig. 2 where we define our notation, with

$$p_i=(p_i^0,\mathbf{p}_i),\quad q=(q^0,\mathbf{q})\ . \tag{5a}$$

We also define

$$\bar{p}_i=(\bar{p}^{\,0}_i,\bar{\mathbf{p}}_i) \tag{5b}$$

as the momentum of the ith outgoing particle. The charge-momentum ratio [Eq. (1)] translates into

$$\frac{Q_1}{p_1\cdot q}=\frac{Q_1}{\bar{p}_1\cdot q}=\frac{Q_2}{p_2\cdot q}=\frac{Q_2}{\bar{p}_2\cdot q}\ . \tag{6}$$

In the e^-p collider, we defined our vectors such that $Q_1=-1$ and $Q_2=-\frac{1}{3}$. The previous equation then leads to

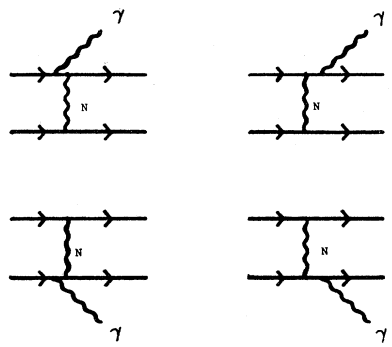

FIG. 1. Feynman diagrams for the processes $e^\pm q\to e^\pm q\gamma$ through $\gamma, Z^0, Z^{0\prime}$ exchange; N stands for any of these gauge bosons. Without any cut, the virtual γ exchange is dominant.

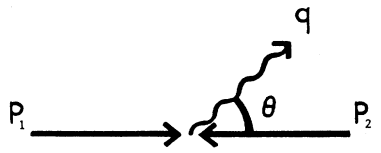

FIG. 2. Definition of the critical angel and related momenta.

$$\cos(\theta_c)=\frac{y-3}{y+3} \tag{7}$$

with $y=p_1^0/p_2^0$. If a radiative zero occurs, it will occur at this critical angle. Table I shows how the critical angle varies as a function of y. This momentum dependence of the critical angle means that unless y is confined to a narrow range, the radiative zero will be "washed out."

As mentioned before, the previous condition positions the dip but does not guarantee its presence. The extra condition imposed to enhance the dip can be written in any frame as

$$R\equiv\frac{Q_i}{Q_j}=\frac{s-2\bar{p}_j^{\,0}\sqrt{s+\mathbf{P}^2}+2\mathbf{P}\cdot\bar{\mathbf{p}}_j}{s-2\bar{p}_i^{\,0}\sqrt{s+\mathbf{P}^2}+2\mathbf{P}\cdot\bar{\mathbf{p}}_i}\ , \tag{8}$$

where $\mathbf{P}=\mathbf{p}_i+\mathbf{p}_j$. In the c.m. frame, $\mathbf{P}=0$ and we recover the well-known result of Eq. (3). With the previous definitions of vectors, this ratio (R) is 3. Again, this extra condition is not essential to destructive interference of different components of the amplitude. If it is not imposed, one should still observe a dip in the differential cross section at the critical angle. Previous numerical calculations often included conditions (7) and (8) in the event generator: all events generated satisfied these conditions exactly. This seems rather extreme since any experimental setup will have to impose these cuts with some uncertainty. In our calculations, we allowed for a range on R and studied how the dip changes as the range is widened or narrowed. This is clearly shown in Fig. 3 for an $e^-(\frac{u}{d})\to e^-\gamma(\frac{u}{d})$ process at 30 GeV per beam. As expected, the dip becomes deeper as the range is narrowed. However, this is accompanied by a drastic loss in cross section, as fewer events have the correct configuration. It is interesting to note that, although it gets deeper, the dip remains rather broad. Also note that the shape of the u-quark process is basically unchanged by the cut; although it also suffers from a large loss in cross section. A range of 1–5 seems to lead to a dip that is not quite at the correct angle. This may be accounted for by a lack of statistics in the Monte Carlo simulation or by the range itself. The smaller range (2–4) certainly leads to the expected dip.

TABLE I. Variation of the critical angle as a function of y.

y	$\cos(\theta_c)$	θ_c (deg)
0.01	−0.99	173
0.1	−0.94	159
1	−0.5	120
2	−0.2	101
3	0	90
10	0.54	57
100	0.94	20

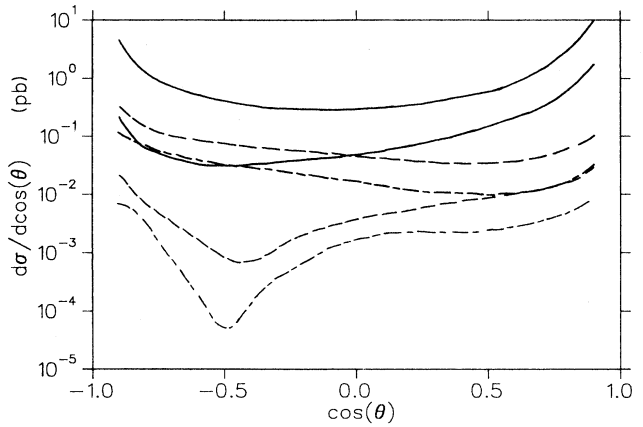

FIG. 3. Angular distribution of the photon for the processes $e^-(\frac{u}{d})\to e^-(\frac{u}{d})\gamma$ at 30 GeV per beam, for different ranges on R. The solid line represents no cut on R, the long dashed line is for $1<R<5$ and the long-short-dashed line corresponds to $2<R<4$. For each pair of lines, the up-quark contribution has the largest cross section. The dip should occur at $\cos(\theta_c)=-0.5$.

Next, we consider beam energies that lead to a dip closer to the beam line: $e^-(\frac{u}{d})$ collision with $2<R<4$ and 30 GeV e^- onto 150-GeV quark. This is shown in Fig. 4. This leads to a very narrow dip since the cross section has to be large at small angle and then must decrease sharply to the dip.

As mentioned before, the momentum dependence of the dip washes it out when one deals with a composite

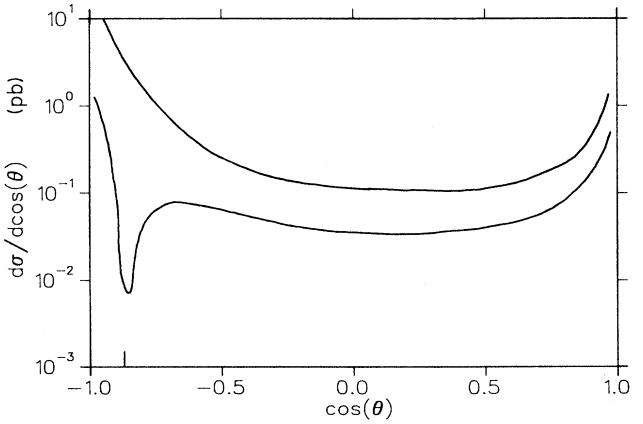

FIG. 4. Angular distribution of the photon for the processes $e^-(\frac{u}{d})\to e^-(\frac{u}{d})\gamma$ at 30-GeV electron beam onto a 150-GeV quark beam. The mark on the horizontal axis indicates where the dip should occur.

object. If one is to observe radiative zeros, one has to extract the parton momentum fraction x and impose some cut on this parameter. In the process at hand, the fact that the photon can radiate from any fermion involved makes the task highly nontrivial. In the following, we will assume that it can be done experimentally. The width and position of the dip at the quark level now lead to useful information. From Fig. 3, we see that the position of the dip ($y=1$ here) should be restricted to the range $-0.6<\cos(\theta_c)<-0.4$ if one is to be left with a well-defined dip. This angular range is reduced to $-0.9<\cos(\theta_c)<-0.85$ for $y=0.2$, as can be seen from Fig. 4. One can relate these limits to a range on x. One obtains

$$-0.6<\cos(\theta_c)<-0.4\ , \qquad 0.073<x<0.125 \tag{9a}$$

and

$$-0.9<\cos(\theta_c)<-0.85\ , \qquad 0.384<x<0.594\ , \tag{9b}$$

where we assumed 30-GeV e^- onto 320-GeV quark. Surprisingly, a narrow dip close to the axis allows a range on the x parameter almost 4 times as large as the range allowed by a broad dip at large angles.

We now turn to the proton processes. We must convolute our parton processes with a momentum distribution function. In general, one has

$$\sigma(e^-p)=\int_{x_{\min}}^{x_{\max}} dx \sum_i q_i(x,P^2)\sigma(e^-q_i)\ , \tag{10}$$

where $q_i(x,P^2)$ is the distribution function for a quark species inside the proton with momentum fraction x and momentum transfer P^2. We used the Eichten-Hinchliffe-Lane-Quigg (EHLQ) distribution[14] function ($n=2$). We used $x_{\min}=0.4$, $x_{\max}=0.6$ and considered a 30-GeV e^- onto a 320-GeV proton beam. However, it is clear, from Figs. 3 and 4 that one should not expect to see a radiative zero in such a collision since the parton that does not lead to a radiative zero is dominant. This is what we see in Fig. 5. We have verified that a polarized e_L^- beam does not change the situation. This result does not agree with another calculation;[15] although the energy range is very different and the analysis differs slightly. From our results, it appears that one will not be able to observe a radiative zero at an e^-p collider.

On the other hand, if one were to use an e^+ beam instead of an e^- beam, one could hope that a dip would remain at the proton level. For the same reason as before (larger range on x) we studied a 30-GeV e^+ beam onto a 150-GeV "quark beam." The range over R was 1–2 ($R=\frac{3}{2}$ here.) The results are shown in Fig. 6. In Fig. 6(a) the two constituents are shown independently, while in Fig. 6(b) we simply add them up as a first, crude approximation to the proton. The results are encouraging since we are left with a wide dip. Note that the asymmetry of the up-quark curve about $\cos(\theta_c)=-0.765$ will shift the dip that arises from the down-quark curve. This is very well seen in Fig. 6(b). In Fig. 7, we show the re-

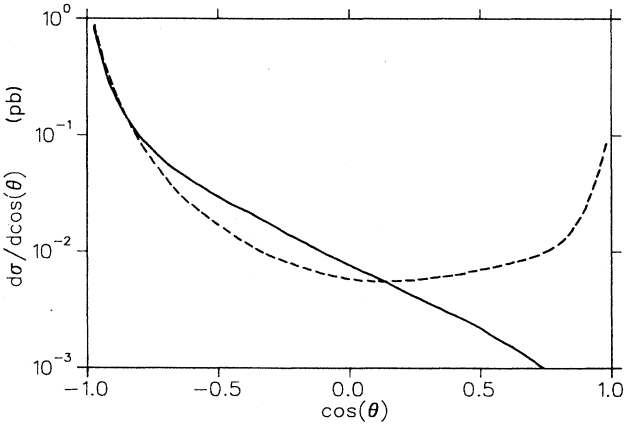

FIG. 5. Angular distribution of the photon and jets in the process $e^-p\to e^-\gamma X$ for a 30-GeV electron beam onto a 320-GeV proton beam. We constrained $0.4<x<0.6$ and $2<R<4$. The photon is given by the dashed line and the jets (X) by the continuous line.

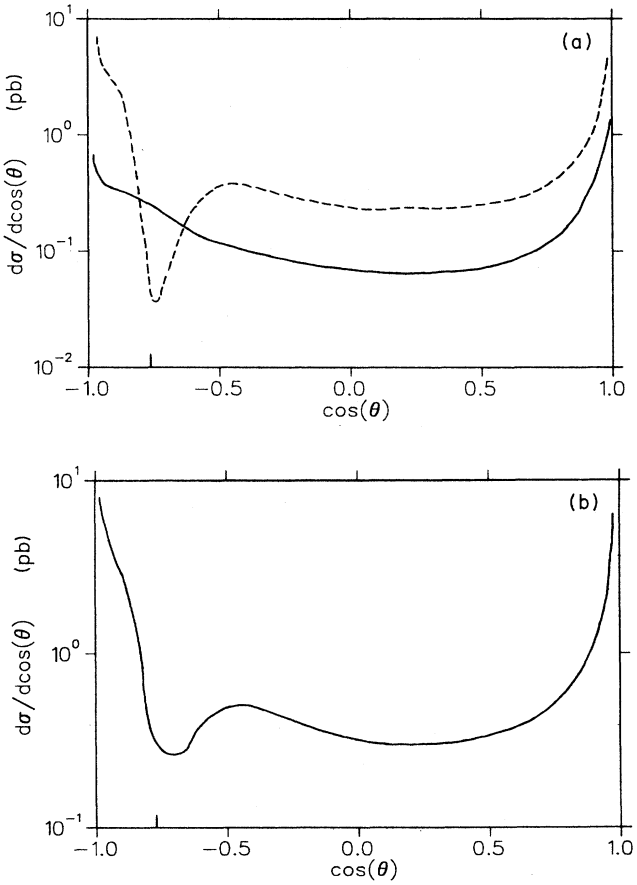

FIG. 6. (a) Angular distribution of the photon in the process $e^+(\frac{u}{d})\to e^+(\frac{u}{d})\gamma$ at 30-GeV positron beam onto a 150-GeV quark beam. The up-quark contribution is given by the dashed line and the down-quark contribution by the solid line. The mark on the horizontal axis indicates where the dip should occur. We imposed $1<R<2$. (b) Summation of the up and down contributions as a first approximation to the proton. Note how the dip is slightly shifted from the critical angle.

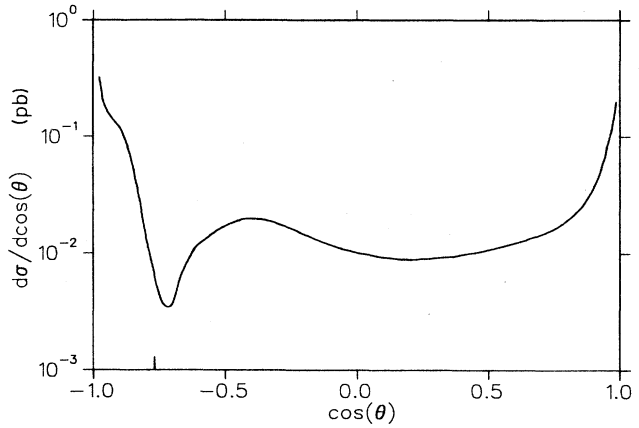

FIG. 7. Angular distribution of the photon in the processes $e^+p \to e^+\gamma X$ at 30-GeV positron beam onto a 320-GeV proton beam with $0.4 < x < 0.6$ and $1 < R < 2$. Note how the dip is slightly shifted from the critical angle.

sults from a 30-GeV e^+ onto a 300-GeV proton with $0.4 < x < 0.6$ and $1 < R < 2$. As expected, the dip is slightly shifted away from the critical angle. The amount by which the dip is shifted would be very difficult to obtain theoretically and would have to be fitted with the data. The same comment applies to the width of the dip.

This last figure is encouraging and shows clearly that once the momentum fraction parameter x can be extracted experimentally, radiative zeros will be observable. However, some more work will be required to obtain the charge of the quark from the position of the dip. This last constraint can be removed if one is willing to work at large angles and under constraint x in a narrower range and suffer further loss in cross section.

III. EXTRA NEUTRAL GAUGE BOSON

In what follows, we give a short review of E_6 considerations relevant to the problem considered; the interested reader is referred to more detailed literature. The notation we used follows closely Ref. 16. E_6 is a rank-6 group; it has six diagonal generators. Two of these are associated with $SU(3)_c$, and two with the electromagnetic and Z^0 charge generators. This leaves two diagonal generators available to extra neutral gauge bosons. Since the U(1) generators of the extra neutral gauge boson must be orthogonal to all generators of the standard model (SM), a convenient labeling is in terms of the subgroup chain:

$$E(6) \to SO(10) \times U(1) \to SU(5) \times U(1)_\chi \times U(1)_\psi ,$$

where the SM is embedded in the SU(5). Then, one can write the Z' charges as a linear combination of the $U(1)_\chi$ and $U(1)_\psi$ charges

$$\begin{aligned} Q' &= Q_\chi \cos(\theta_{E_6}) + Q_\psi \sin(\theta_{E_6}) , \\ Q'' &= -Q_\chi \sin(\theta_{E_6}) + Q_\psi \cos(\theta_{E_6}) . \end{aligned} \tag{11}$$

The specific value of the mixing angle θ_{E_6} will depend on the symmetry-breaking scheme. In the previous notation, $\theta_{E_6} = 0$ corresponds to the extra Z^0 in SO(10), $\theta_{E_6} = 90$ corresponds to the extra Z^0 in E_6. We assume here that if two extra neutral gauge bosons appear, one will be massive enough to be irrelevant to our problem; as we will see, 1 TeV/c^2 is sufficient. The different couplings of this extra gauge boson to the different fermions are given in Table II. We write the effective neutral-current Lagrangian as

$$L_{NC} = -e A_\mu J^\mu_{em} - g_{Z^0} Z^0_\mu J^\mu_{Z^0} - g_{Z'} Z'_\mu J^\mu_{Z'} \tag{12}$$

with the currents $J^\mu = \sum_f C^f_L \bar{f} \gamma^\mu f$.

Since this Z' has same quantum numbers as the SM Z^0, there will be mixing, parametrized by the mixing angle ϕ. The physical fields Z^0_p and Z'_p are now combinations of the gauge fields Z^0 and Z'. This mixing will also change the fermion couplings; they now read

$$\begin{aligned} C_{L,R} &= C^{SM}_{L,R} \cos(\phi) + (g_{Z'}/g_{Z^0}) C^{E_6}_{L,R} \sin(\phi) , \\ C'_{L,R} &= -(g_{Z'}/g_{Z^0}) C^{SM}_{L,R} \sin(\phi) + C^{E_6}_{L,R} \cos(\phi) , \end{aligned} \tag{13}$$

where $C^{SM}_{L,R}$ are the SM couplings. The mixing angle ϕ can be related to the physical states via matrix diagonalization:

$$\tan^2(\phi) = \frac{M^2_{SM} - M^2_{Z^0_p}}{M^2_{Z'_p} - M^2_{SM}} . \tag{14}$$

Therefore, accurate mass measurements could determine ϕ. However, we will treat it as a free parameter. Furthermore, renormalization-group arguments constraint $(g_{Z'}/g^{Z^0})^2 \leq \frac{5}{3}\sin^2(\theta_W)$, the exact value being strongly

TABLE II. Couplings of the E_6 Z boson to the fermions.

Fermion	$C^{E_6}_L$	$C^{E_6}_R$
l	$\frac{3}{2\sqrt{10}}\cos\theta_{E_6} + \frac{1}{2\sqrt{6}}\sin\theta_{E_6}$	$\frac{1}{2\sqrt{10}}\cos\theta_{E_6} + \frac{1}{2\sqrt{6}}\sin\theta_{E_6}$
ν	$\frac{3}{2\sqrt{10}}\cos\theta_{E_6} + \frac{1}{2\sqrt{6}}\sin\theta_{E_6}$	$\frac{5}{2\sqrt{10}}\cos\theta_{E_6} + \frac{1}{2\sqrt{6}}\sin\theta_{E_6}$
u	$-\frac{1}{2\sqrt{10}}\cos\theta_{E_6} + \frac{1}{2\sqrt{6}}\sin\theta_{E_6}$	$\frac{1}{2\sqrt{10}}\cos\theta_{E_6} + \frac{1}{2\sqrt{6}}\sin\theta_{E_6}$
d	$-\frac{1}{2\sqrt{10}}\cos\theta_{E_6} + \frac{1}{2\sqrt{6}}\sin\theta_{E_6}$	$-\frac{1}{2\sqrt{10}}\cos\theta_{E_6} + \frac{1}{2\sqrt{6}}\sin\theta_{E_6}$

model dependent. For simplicity, we assumed the equality.

From the preceding lines, it is clear that there is a lot of freedom in these models with several free parameters. Over the past two years or so, numerous authors have tried to constrain these models from neutral-current data, atomic parity measurements, Drell-Yan production at UA1 and UA2, and others. Again, the interested reader is referred to the detailed literature.[17] As a rule, the lower bounds on the mass of an extra Z boson from these processes show a strong dependence on θ_{E_6}. Only the UA1-UA2 data is almost θ_{E_6} independent and sets a lower bound of ~ 150 GeV/c^2 on the mass of an extra neutral gauge boson produced via the Drell-Yan mechanism. Other bounds vary from 0 to 500 GeV/c^2, depending on θ_{E_6}. Given this, we decided on a lower bound of 150 GeV/c^2 and set $\theta_{E_6}=90$ for our numerical calculation.

From another point of view, one can try to constrain the mass and the mixing angle ϕ. Such considerations lead to loose bounds on the mass but constrain ϕ to a small range: $-0.25<\phi<0$. Future experiments should bring the lower bound to -0.05. For simplicity, we set the mixing angle ϕ to be 0.

With this set of parameters, we study the same processes:

$$e^{\pm}p \to e^{\pm}\gamma X, \quad e_L^- p \to e_L^- \gamma X \ .$$

As the processes can proceed via photon exchange, we have to impose a cut in order to enhance the presence of a heavy boson. In fact, from QED, one expects the differential cross section to become very large at small angles. Because we require that all particles be seen, we impose a 5° cut since, from an experimental point of view, detection close to the beam line is very difficult. Obviously, this cut will not enhance the effect of a massive gauge boson; the photon exchange with small momentum transfer will still dominate the process. However, we can impose a large momentum transfer in order to reduce the photon contribution and increase the effect of a massive neutral gauge boson. Admittedly, the cross section will be reduced. As we started with a very large rate, we hope to be left with a rate that is measurable.

Consider Fig. 8, where our notation is defined: the goal is to impose a cut that does not involve the quark legs, as they are difficult to tag experimentally. If the photon comes off the quark legs, the photon momentum is $(p'-p)^2$; while it is $(p-p'-k)^2$ when the photon comes off a lepton leg. Therefore, we impose

$$-(p'-p)^2 > fM_Z^2 \quad \text{and} \quad -(p-p'-k)^2 > fM_Z^2 \ , \tag{15}$$

where f is a number greater than 0. We want to tune f in order to get the largest mass effect and be left with the largest cross section. This was done by trial and error. It appeared that $f \approx 0.2$ gave the best results. The optimal value is not sharply defined, but $f=0.05$ or $f=0.5$ are certainly not as good as $f=0.2$. Note that this cut requires very high beam energies. As the overall cross section scales as $(1/s)^2$ (Ref. 15), one would be tempted to reduce the energy. However, at low energy (say an order of magnitude less), the cut will reduce the cross section too much and the enhanced effect of a massive gauge boson will be lost in the statistical error of any foreseeable accelerator.

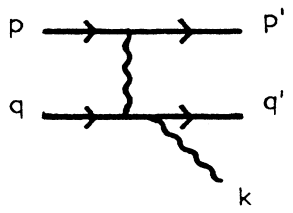

FIG. 8. Notation on the cuts imposed in order to enhance the effect of a massive gauge boson.

TABLE III. Different cross sections as a function of the proton energy for a given electron energy of 30 GeV. We used $f=0.2$ and $x_{\min}=0.001$. Note $\sigma_{\bar{\omega}}$ is the cross section given a mass of $\bar{\omega}$ for the extra gauge boson. Δ is the experimental statistical error one can expect for σ_{1000} for the given luminosity. We used a fine-structure constant α of $\frac{1}{128}$, $\sin^2(\theta_W)=0.23$, and $M_Z=93$ GeV/c^2.

	P_p (GeV)			$\int \mathcal{L}\, d\tau$
	350	500	820	(pb^{-1})
$\sigma_{150}/\sigma_{1000}$	0.965	0.966	0.970	
$\sigma_{400}/\sigma_{1000}$	0.994	0.994	0.995	
σ_{1000} (pb)	2.2	3.4	5.4	
Δ	0.055	0.044	0.035	150
Δ	0.028	0.022	0.018	600
Δ	0.022	0.018	0.014	900

In Tables III, IV, and V, we present our results for different values of the proton beam energy and a given lepton energy of 30 GeV. We have set $f=0.2$ in all of these. We present the results as ratios of cross sections with respect to the cross section where the extra neutral gauge boson has a mass of 1 TeV. This last value σ_{1000} is essentially the SM cross section since such a massive

TABLE IV. Different cross sections as a function of the proton energy for a given positron energy of 30 GeV. Same set of parameters as for Table III.

	P_p (GeV)			$\int \mathcal{L}\, d\tau$
	350	500	820	(pb^{-1})
$\sigma_{150}/\sigma_{1000}$	0.970	0.973	0.978	
$\sigma_{400}/\sigma_{1000}$	0.995	0.993	0.995	
σ_{1000} (pb)	1.7	3.1	4.7	
Δ	0.063	0.046	0.038	150
Δ	0.031	0.023	0.019	600
Δ	0.026	0.019	0.015	900

TABLE V. Different cross sections as a function of the proton energy for a given left-handed electron energy of 30 GeV. Same set of parameters as for Table III.

	P_p (GeV)			$\int \mathcal{L}\, d\tau$
	350	500	820	(pb^{-1})
$\sigma_{150}/\sigma_{1000}$	0.98	0.98	0.984	
$\sigma_{400}/\sigma_{1000}$	0.997	0.997	0.997	
σ_{1000} (pb)	2.2	3.6	5.4	
Δ	0.055	0.043	0.035	150
Δ	0.028	0.022	0.018	600
Δ	0.022	0.018	0.014	900

gauge boson has no measurable effects on the rate. The last lines of the tables, Δ, are the experimental statistical errors one can expect from σ_{1000} using luminosities in the range of the HERA machine.[18] It seems that the highest luminosity will be available for a proton beam energy of 500 GeV or less. The highest beam energy will have an integrated luminosity of 150 pb^{-1}. Then in the following analysis, we will use these values and consider the other results for completeness.

Consider first the e^-p case. We see that the effect is maximum with a 500-GeV proton beam: we have more than a 2-standard-deviation (SD) effect from a light extra gauge boson. Higher energies are plagued by small luminosities and the effect reduces to less than 1 SD. This compares with other experiments at future colliders (see, for example, Refs. 16 and 17). One could also invert the argument and calculate the required luminosity to get a 1-SD effect given the cross section; one obtains ~ 250 pb^{-1}. This value seems within the designed range of the machine. It is clear that an e^+ beam cannot do any better than the e^- beam. It is interesting to note here that from QED alone, one would expect $\sigma(e^-p \to e^-\gamma X) = \sigma(e^+p \to e^+\gamma X)$ since the corresponding couplings for the two processes have the same magnitude. However, the Z and Z' spoil the symmetry and the results now slightly differ. At higher energies, the cut we impose becomes less efficient and the photon again dominates. As a result, the two cross sections become similar. In principle, one could use this difference to study the g_v and g_a couplings of the bosons. Finally, we see that the polarization of the e^- beam does not help. The cross sections are very similar, but the amplitude of the effect decreases. Experimentally, the polarization at HERA is 80–85 %; and the error on this value would be sufficient to erase the small effects we have seen. One would most likely rely on an unpolarized electron beam. The main point here is that a 150-GeV extra neutral gauge boson can lead to a 2-SD effect at an e^-p collider. On the other hand, a 400-GeV boson leads to a 0.5-SD effect and most likely would be unnoticed. Realistically, the maximum mass one can probe via the process at hand seems to be 250–300 GeV; at the 1-SD level. This compares well with other processes and has the advantage of having $\phi = 0$, so that the minimum mass obtained from such an experiment would be an absolute minimum, irrespective of the mixing.

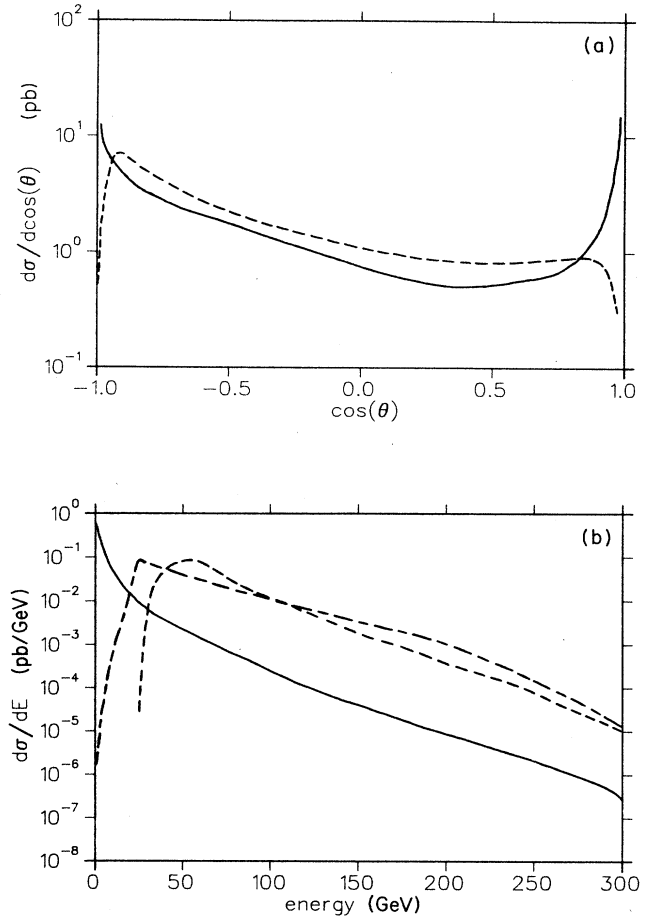

FIG. 9. (a) Angular distribution of the outgoing particles in the process $e^-p \to e^-\gamma X$ at 30-GeV electron beam onto a 500-GeV proton beam. We used $f = 0.2$ and $x_{\min} = 0.001$ and a 1-TeV/c^2 extra neutral gauge boson. The solid line represents the photon while the dashed line is for the jets. (b) Energy distributions of the outgoing particles in the process $e^-p \to e^-\gamma X$ with the same set of parameters as in (a). The solid line is for the photon, the long-short-dashed line is for the jets, and the dashed line is for the electron.

In Fig, 9, we present different distribution for the most promising set of parameters. From Fig. 9(a), it is clear that most particles go in the proton direction, which is expected. This would make the tagging of the photon very difficult since it would be surrounded by the jets. However, a large fraction of the photons emitted in the process go along the direction of the initial lepton; where there are not very many hadrons and no lepton whatsoever. One should then be able to detect the photon easily, at the cost of sacrificing half of the cross section. Furthermore, Fig. 9(b) shows that the photons we are interested in are very-low-energy ones. In fact, the cut we imposed on the photon energy (0.5 GeV) is rather conser-

vative. The cross section can be doubled, roughly, if one can reduce the cut to 0.25 GeV, gaining back the factor of 2 lost in the backward direction. Note also that the amount of energy in the jets is quite large compared to the photon energy. These two distributions (angular and energy) give some indication that a potentially very large background might be avoided. As we destroy the proton, we expect a lot of hadrons to be produced; among these π^0's. This hadron decays into a pair of photons in $\sim 10^{-16}$ sec. At the energies considered here, the two photons would be almost collinear, in the original direction of the π^0 and they should share the energy equally. From Figs. 9(a) and (9b) it seems one could be able to avoid this background almost completely by selecting energies and angles. On the other hand, the distributions change so little with the mass of the extra gauge boson that one would have to consider the whole integrated cross section in order to put a bound on the mass. Furthermore, we looked at the transverse momentum distribution of the scattered quark. We found a broad distribution ranging from 0 to 120 GeV, peaking at ≈ 50 GeV and decreasing sharply below 5 GeV or above 90 GeV. From this distribution, we could see that imposing a cut of 20 GeV on the transverse momentum of the scattered quark would not reduce the cross section by much; less than 20%. This cut is relevant for radiative zeros as it would allow a measurement of the energy of the scattered quark, which then could lead to a measurement of the parton momentum fraction x.

IV. SUMMARY AND CONCLUSIONS

We have studied the process $e^{\pm}p \to e^{\pm}\gamma X$ and considered the possibilities of observing radiative zeros or extra neutral gauge bosons. We have seen that it will be impossible to observe radiative zeros at e^-p colliders because the up-type quarks do not lead to radiative zeros while accounting for most of the cross section. On the other hand, e^+p colliders will lead to radiative zeros under the strong constraints of being able to extract the momentum fraction parameter x and impose some cuts upon it. Even then, the more useful information, the charge of the quark, will be difficult to extract from the position of the dip. Indeed, we have seen that the dip can be shifted away from its position at small angles, due to some asymmetries in the angular distributions of the up- and down-type quarks. This asymmetry can be avoided if one is willing to consider larger angles but much smaller ranges of the momentum fraction parameter.

On the other hand, our results are encouraging as far as extra neutral gauge bosons are concerned. Using current parameters of the HERA machine, we have seen that an extra gauge bosons can lead to a 2-standard-deviation effect. This compares favorably with other experiments at colliders. The enhancement requires very good tagging and tracking of the outgoing electron and photon. This experiment could lead to a very strong constraint on the mass of a neutral gauge boson considering that we used a mixing angle ϕ of 0. Again, it is worthwhile to mention that the numbers obtained here are based on a conservative photon energy cut. The cross section can be enhanced greatly ($\sim 2-3$) by reducing the minimum energy of the photon in half. Therefore, it appears that a tight bound on the mass of an extra neutral gauge boson can be obtained from the process at hand.

A last remark concerns the process $e^-p \to e^-p\gamma$. It will be used at the HERA machine to monitor the luminosity of the beams. The theoretical expectations for that process in some specific angular and energy ranges have been very well known for a long time[19] and some beam size effects can be taken into account if necessary.[20] Obviously, this process requires very low momentum transfer since the proton must not be broken or excited. Therefore, one searches for low-energy photons very close to the beam line. As we imposed a 5° cut and required rather large momentum transfer in order to enhance the effect of a massive gauge boson, the presence of such a boson would be of no consequence to the monitoring process.

ACKNOWLEDGMENTS

I wish to thank J. Davis and his group whose microvax I have been using. I also benefited from discussions with S. Godfrey. This research was supported by the Natural Sciences and Engineering Research Council (NSERC) of Canada under Grant No. UO573.

---

*Present address: Brookhaven National Laboratory, Upton, NY 11973.

[1]R. J. Cashmore *et al.*, Phys. Rep. **122**, 275 (1985); E. Gabrielli, World Phys. Lett. A **1**, 465 (1986).

[2]G. Wolf, in *First Aspen Winter Physics Conference, 1985,* edited by M. M. Block (Ann. N.Y. Acad. Sci. No. 461) (New York Academy of Sciences, New York, 1986), p. 699.

[3]G. Ingelman and R. Rückl, Phys. Lett. B **201**, 369 (1988).

[4]S. Dimopoulos, Nucl. Phys. **B168**, 69 (1980); E. Fahri and L. Susskin, Phys. Rev. D **20**, 3404 (1979); see also Ref. 1 for phenomenology.

[5]S. Godfrey, Phys. Lett. B **195**, 78 (1988).

[6]F. Cornet, in *Lepton Nucleon Interactions at High Energies,* proceedings of the XVth International Winter Meeting on Fundamental Physics, Seville, Spain, 1987, edited by F. Barreiro and J. L. Sanchez-Gomez (World Scientific, Singapore, 1988), p. 209; S. Capstick and S. Godfrey, Phys. Rev. D **35**, 3351 (1987).

[7]K. O. Mikaelian, M. A. Samuel, and D. Sahdev, Phys. Rev. Lett. **43**, 746 (1979); A. J. H. Reid, M. A. Samuel, and G. Tupper, Prog. Theor. Phys. Lett. **74**, 1356 (1985); M. A. Samuel and J. H. Reid, *ibid.* **76**, 184 (1986); R. W. Brown, D. Sahdev, and K. O. Mikaelian, Phys. Rev. D **2**, 1164 (1979); L. Hagiwara, F. Halzen, and F. Herzog, Nucl. Phys. **B135**, 324 (1984).

[8]G. Couture and J. N. Ng, Z. Phys. C **35**, 65 (1987); G. Couture, J. N. Ng, J. L. Hewett, and T. G. Rizzo, Phys. Rev. D **36**, 859 (1987); G. Couture, J. N. Ng, J. L. Hewett, and T. G. Rizzo

(unpublished); C. L. Bilchak, R. Gastmans, and A. van Proyen, Nucl. Phys. **B273**, 46 (1986).

[9]J. Cortes, K. Hagiwara, and F. Herzog, Nucl. Phys. **B278**, 26 (1984).

[10]S. L. Brodsky and R. W. Brown, Phys. Rev. Lett. **49**, 966 (1982).

[11]R. W. Brown, K. L. Kowalski, and S. J. Brodsky, Phys. Rev. D **28**, 624 (1983).

[12]Compare G. Couture and J. N. Ng, Z. Phys. C **32**, 579 (1986), and H. Neufeld, *ibid.* **17**, 145 (1983).

[13]F. A. Berends *et al.*, Nucl. Phys. **B103**, 124 (1981).

[14]E. Eichten, J. Hinchliffe, K. Lane, and C. Quigg, Rev. Mod. Phys. **56**, 579 (1984).

[15]M. A. Samuel and J. Reid, Phys. Rev. D **35**, 3505 (1987); **36**, 3527(E) (1987); **38**, 2913(E) (1988). Note that Eqs. (3)–(6) of Hagiwara *et al.* in Ref. 7 and Eqs. (5)–(8) of Ref. 15 lead to a cross section with wrong dimensionality. It also appears that some quark and lepton charges squared are missing in Eq. (7) of Ref. 15.

[16]S. Capstick and S. Godfrey, Phys. Rev. D **37**, 2466 (1988).

[17]J. F. Gunion, in *Superstrings, Cosmology, and Composite Structures,* proceedings of the International Workshop, College Park, Maryland, 1987, edited by S. J. Gates, Jr. and R. N. Mohapatra (World Scientific, Singapore, 1987), p. 333; V. Barger and K. Whisnant, Int. J. Mod. Phys. A **3**, 879 (1988); N. G. Deshpande, in *Physics at Future Accelerators,* proceedings of the X Warsaw Symposium on Elementary Particle Physics, Kazimierz, Poland, 1987, edited by Z. Ajduk (Warsaw University, Warsaw, 1987), p. 575; L. S. Durkin and P. Langacker, Phys. Lett. **166B** , 436 (1986); U. Amaldi *et al.*, Phys. Rev. D **36**, 1385 (1987).

[18]Particle Data Group, M. Aguilar-Benitez *et al.*, Phys. Lett. **170B**, 1 (1986).

[19]H. Bethe and W. Heitler, Proc. R. Soc. London **A146**, 83 (1984).

[20]G. L. Kotkin, S. I. Polityko, A. Schiller, and V. G. Serbo, Novosibirsk State University report (unpublished).